Results in Chemistry 7 (2024) 101544

Contents lists available at ScienceDirect

Results in Chemistry

journal homepage: www.sciencedirect.com/journal/results-in-chemistry

Evaluation of the binding efficacy of flavonol derivatives on estrogen receptors (ER) with respect to ring B hydroxylation

K.P Safna Hussan [a,b,*,1], Anu Davis [a,1], S. Lekshmi [c], Mohamed Shahin Thayyil [d], Achuthan Chathrattil Raghavamenon [a], Thekkekara Devassy Babu [a,*]

[a] Department of Biochemistry, Amala Cancer Research Centre, Amalanagar P O, Thrissur - 680 555, Kerala, India
[b] Ayurgreen Scientifica Research Institute, Ayurgreen Campus, Kavilpadi, Kaladi, Malappuram - 679 582, Kerala, India
[c] Department of Physics, Sanatana Dharma College, Alapuzha - 688 003, Kerala, India
[d] Department of Physics, University of Calicut, Malappuram - 673 635, Kerala, India

ARTICLE INFO

Keywords:
Estrogen Receptors
Flavonol derivative
Density Functional Theory
Molecular Docking

ABSTRACT

Rationale: Flavonols are a class of flavonoids, consist of two aromatic rings (A and B) connected by a three-carbon bridge, forming a closed pyran ring (C) with a hydroxyl group at position 3. Galangin is a form of flavonols formed with additional hydroxyl groups at ring A positions 5 and 7. The hydroxylation at ring B of galangin may result in resonance and delocalization of electrons and the formation of different derivatives like kaempferol, quercetin, and myricetin. Most of these flavonols have a similarity to 17β-estradiol, the steroid sex hormone which bound to estrogen receptors (ER), a class of nuclear transcription factors involved in the regulation of many complex pathophysiological processes including breast cancer genesis and progression. Various studies have reported that most of the flavonols are antiestrogenic and show anticancer potential, but the mechanisms may be varied like estrogenic, anti-estrogenic, non-estrogenic, and biphasic activities and their mechanisms of action have not been systematically evaluated.

Aim: The goal of this study is to ascertain the possible interactions of flavonol derivatives to ER with respect to ring B hydroxylation and the unsaturation degree of the C2′=C3′ bond.

Methods: The variations in structure, frontier molecular orbital, molecular electrostatic potential maps, Mullikan charge population of derivatives was determined by Density functional theory (DFT) calculations at B3LYP/6-311G (d,p) level on model molecular systems. A deep insight into these interactions with ER was described by molecular docking studies.

Results and discussion: Results shows that the flavonol was found more affinity to ERβ and the efficacy was increased with respect to the OH group on ring B. The hydroxyl group at position 3 and 5 in ring A and C are not found much relevant. The site of ERβ is more hydrophilic while binding ligand and the electropositive and electronegative area of the molecule was increased and reaches a maximum for quercetin with the 3 OH group; after that, it found to diminish. Moreover, the reduced cavity size of ERβ and the replacement of LEU384 with polar HIE475 and MET336 increased the polarity and hydrophilicity of the cavity and led to more electrostatic interaction with ligands. ERα is found to be hydrophobic and the polar interaction between the ligands and ERα is less due to open confirmation of the cavity and bulk empty space. The results also emphasize that myricetin and quercetin require less energy to activate while accounting for the values of Gibbs free energy, the electronic configuration of frontier molecular orbitals, and entropy.

Conclusion: The hydroxylation on ring B has a significant importance in the chemical reactivity as well as estrogenic activity of flavonol.

* Corresponding authors at: Ayurgreen Scientifica, Ayurgreen Hospital Campus, Kavilpadi, Kaladi, Malappuram 679 582, Kerala, India (K.P Safna Hussan).
E-mail addresses: safnahussain2@gmail.com (K.P Safna Hussan), babutharakan@gmail.com (T. Devassy Babu).
[1] These authors equaly contribute to this work and shares first authorship.

https://doi.org/10.1016/j.rechem.2024.101544
Received 19 March 2024; Accepted 13 May 2024
Available online 14 May 2024

Introduction

The phenolic molecules, which range widely in size and complexity, ranging from tiny, low-molecular-weight, single aromatic-ringed molecules to massive, complex tannins and derived polyphenols make up a broad class of secondary metabolites present in plants [1]. They are categorised according to the quantity and arrangement of their carbon atoms and are distinguished by possessing at least one aromatic ring to which one or more hydroxyl (OH) groups are linked. Phenols are divided into two important categories: flavonoids and non-flavonoids. They frequently occur conjugated with organic acids and sugars. Among these, flavonoids are widespread and the most numerous group of molecules. Studies have demonstrated that flavonoids possess various biological and pharmacological properties, including antioxidant, cytotoxic, anticancer, and anti-inflammatory effects [2 3]. Most of these flavonoids bear similarities to 17β-estradiol, the steroid sex hormone that binds to estrogen receptors (ER), a class of nuclear transcription factors tangled in the directive of several complex pathophysiological processes, including breast cancer genesis and progression. Consequently, phytoestrogenic flavonoids interact with ER and can mimic, modulate, or block the effects of endogenous estrogens, thereby influencing gene expression, cellular signaling, and physiological responses.

Phytoestrogens are generally considered to have a weaker affinity for ER than 17β-estradiol and may have different effects in different parts of the body. By binding to ER, phytoestrogens prevent or reduce the binding of estradiol, thus modulating the estrogenic effects. Flavonoids have been found to interfere with estrogen-mediated cellular signaling pathways. They may alter gene expression, obstruct cell proliferation, and prompt apoptosis in estrogen-sensitive cells. Some may inhibit the aromatase enzyme activities liable for altering androgens to estrogens. The antiestrogenic properties of flavonols have sparked interest in their potential role in sinking the threat of hormone-related melanomas like breast, prostate, and ovarian cancers [2 4]. The effects may differ depending on factors such as the phytoestrogen type, dose, alterations in metabolism, and cancer types. Several flavonoids have been reported to have a tendency to induce proliferation in ERα positive breast cancer cells, such as MCF7 [5]. Galangin, one of the bioflavonoids, is found to inhibit the growth of ER-negative cell lines like Hs578T and down-regulate cyclin D3, E, and A [6]. Resende et al. reported that quercetin, chrysin, and 3-hydroxyflavone act as ER antagonists since they significantly inhibited the cell proliferation of MCF7/BUS in the E-screen assay [7]. Kuiper reported that Certain phytoestrogens compete more vigorously with estradiol for binding to ERβ than ERα, including coumestrol, genistein, apigenin, naringenin, and kaempferol [8]. Thus, the effects of phytoestrogens become ambiguous due to various mechanisms like estrogenic, antiestrogenic, non-estrogenic, and biphasic activities depending on tissues and other pathophysiological conditions [9].

Considering the differential nature of the wide range of flavonoid phytoestrogens, the current research gives priority to flavonols, consisting of two aromatic rings (A and B) connected by a three-carbon bridge that forms a closed pyran ring (C) with a hydroxyl group at position 3 [10 11]. Galangin, one of the form of flavonols formed with additional hydroxyl groups at positions 5 and 7 of ring A (Fig. 1). Other flavonols, including kaempferol, quercetin, and myricetin, differ based on the number and placement of hydroxyl groups on ring B of galangin. Specifically, kaempferol has a single hydroxyl group at the 4′ position, quercetin has two hydroxyl groups at the 3′ and 4′ positions, and myricetin features three hydroxyl groups at the 3′, 4′, and 5′ positions. The hydroxylation at the ring B may result in a resonance and delocalization of electrons and the formation of different derivatives. The study is attempted to correlate the possible interactions of flavonol derivatives to ER with respect to ring B hydroxylation.

Materials and methods

The input structures were the drugs; flavone ($C_{15}H_{10}O_2$) with mol. wt of 222.24 g/mol (PubChem: 10680), chrysin ($C_{15}H_{10}O_4$) with mol. wt of 254.24 g/mol (PubChem: 5281607), galangin ($C_{15}H_{10}O_5$) with mol. wt of 270.24 g/mol (PubChem: 5281616), kaempferol ($C_{15}H_{10}O_6$) with mol.wt of 286.24 g/mol (PubChem: 3394), quercetin ($C_{15}H_{10}O_7$) with mol.wt of 302.03 g/mol (PubChem: 5280343), myricetin ($C_{15}H_{10}O_8$) with mol. wt of 318.23 g/mol (PubChem: 5281672) were taken from the PubChem database [12] which were in SDF (Standard Data File) format and were converted to GJF (Gaussian Job File) input files using the application Open Babel [13].

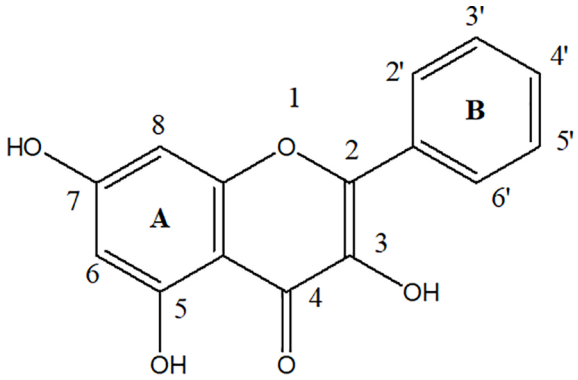

Fig. 1. Structure of galangin.

Computational details

All the quantum calculations were performed by density functional theory using a Gaussian 09 software package [14]. The initial geometries selected from the PubChem database were optimized using the B3LYP/6–311++G (d,p) level of the theory [12]. The Lee, Yang Parr (LYP) functional and the exchange and electronic correlation terms in DFT are added using Becke's three-parameter practical hybrid technique, or B3LYP. The optimized geometry was correlated to crystallographic data in the Cambridge Crystallographic Data Center, such a assessment between the experimental and theoretical values facilitated to lessen the error in the optimized geometry. The optimized geometry was castoff for the calculations of harmonic vibrational frequencies at the B3LYP/6–311++ G (d,p) method, it also aided to warrant the structures to be global minima. The parameters of thermochemistry [15–17] such as chemical potential (μ), electronegativity (χ), softness (S), hardness (η), and electrophilicity index (ω), were calculated using Koopman's theorem for closed-shell compounds. Analysis of electrostatic potential was done to determine the drug's mapping surface [16–21].

Supplementary, molecular docking was also performed to forecast binding positions, bio affinity, and virtual screening of the nominated drugs into the 3D crystal structure of ERα (PDB ID: 1A52) and ERβ (PDB ID: 3OLL) using GLIDE Dock Program in Schrödinger Maestro software. The protein preparation wizard, which used under-restrained minimization and the OPLS 2003 force field to constrain heavy atoms, was utilised to improve the protein structure. The ligands were chanced to ligand preparation by the ligand preparation wizard (Lig prep) of Schrödinger software in the Maestro interface (11.5). The grid center were utilised to describe the active location and case sizes to 20 Å [22–24].

Results

Molecular geometry

The optimized molecular geometries of a) flavone, b) chrysin, c) galangin d) kaempferol/robigenin e) quercetin, and f) myricetin were evaluated using B3LYP/6–311++G (d,p) level of the theory and

depicted in Fig. 2. The molecular configuration of flavone was minimised to the global minima with potential energy -4.56×10^5 kcal/mol, chrysin to -5.51×10^5 kcal/mol, galangin to -5.98×10^5 kcal/mol, kaempferol to -6.46×10^5, quercetin to -6.93×10^5 and myricetin to -7.40×10^5 kcal/mol. The bond lengths and angles are tabulated in Table 1. Compare to flavones structural parameters, chrysin have additional hydroxyl groups at 26O-27H and 28O-29H with bond length 0.963, in order to these hydroxylations the bondlength of A ring has substantial change as shown in Fig. 2. Similarly galangin B has undergone hydroxylation at third position with a weak OH bond of length 0.983 with no visible change in other bonds. In the case of flavonols, B-ring does not share the same plane as the AC-complex. Depending on the intramolecular repulsions or hydrogen bonding resulting from C3, C2′ or C5′ residues [25]. Quercetin exists as hydrogen-bonded dimers packing almost perpendicular to c.

Thermo-chemical properties

The computationally calculated thermochemical parameters are given in Table 2, these parameters will help us to determine the most stable phytochemical compound under study depending on the value of enthalpy (H), entropy (S), and Gibbs free energy (G). In general, the more negative value of G and more positive entropy value determines the most active chemical compound. From the investigation, it is observed that myricetin has a more negative value for G (-7.41×10^5 kcal/mol) and flavone has more or less the same G value (-4.568×10^5 kcal/mol). In that sense, myricetin is a chemically more active molecule than others. It is interesting to note that on hydroxylation of flavone, the chemical activity of the molecule increases with an increase in the number of OH functional groups.

The deviations, which represent changes in thermodynamic parameters upon hydroxylation at ring B of the respective flavonoid compounds, were tabulated in Table 2. These insights shed light on the

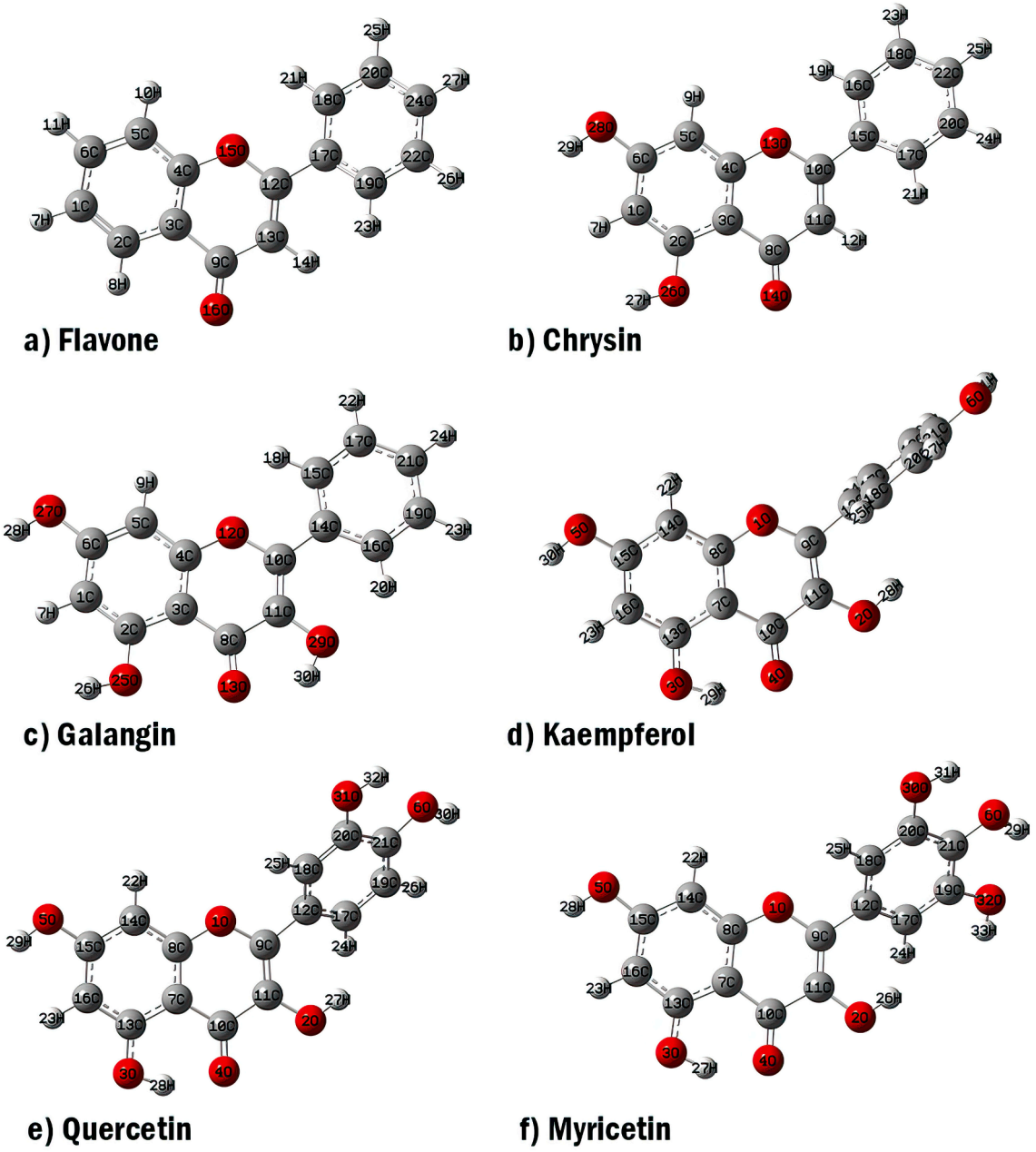

Fig. 2. The optimized molecular geometries of the selected flavonols, calculated at DFT/B3LYP/6311++ G (d,p).

Table 1
The bond length of optimized molecular structures of the selected flavonols, calculated at DFT/B3LYP/6311++ G (d,p).

	Flavone	Chrysin	Galangin	Myricetin	Quercetin	Kaempferol
C1-C2	1.384	1.393	1.388	1.390	1.390	1.390
C1-C6	1.402	1.399	1.404	1.400	1.400	1.400
C1-H7	1.084	1.087	1.087	1.084	1.084	1.084
C2-C3	1.402	1.418	1.420	1.424	1.424	1.425
C2-H8	1.083	1.351	1.350	1.336	1.336	1.336
C3-C4	1.397	1.407	1.410	1.404	1.404	1.406
C3-C9	1.482	1.482	1.453	1.448	1.448	1.449
C4-C5	1.396	1.391	1.393	1.387	1.387	1.388
C4-O15	1.372	1.369	1.354	1.363	1.362	1.363
C5-C6	1.386	1.388	1.386	1.395	1.395	1.394
C5-H10	1.083	1.081	1.081	1.081	1.081	1.081
C6-H11	1.084	1.359	1.358	1.359	1.359	1.359
C9-C13	1.456	1.464	1.472	1.463	1.463	1.465
C9-C13	1.456	1.464	1.472	1.463	1.463	1.465
C12-C13	1.355	1.349	1.360	1.363	1.363	1.356
C12-O15	1.363	1.365	1.378	1.369	1.370	1.370
C12-C17	1.475	1.475	1.467	1.472	1.472	1.483
C13-H14	1.081	1.080	1.350	1.363	1.361	1.359
C17-C18	1.403	1.402	1.407	1.400	1.405	1.403
C17-C19	1.403	1.403	1.407	1.408	1.402	1.399
C18-C20	1.391	1.391	1.389	1.391	1.385	1.387
C18-H21	1.082	1.082	1.081	1.081	1.082	1.084
C19-C22	1.389	1.389	1.390	1.390	1.395	1.391
C19-H23	1.083	1.083	1.079	1.084	1.083	1.084
C20-C24	1.393	1.393	1.393	1.398	1.407	1.398
C20-H25	1.084	1.084	1.084	1.357	1.358	1.083
C22-C24	1.394	1.394	1.393	1.394	1.387	1.397
C22-H26	1.084	1.084	1.084	1.373	1.086	1.086
C24-H27	1.084	1.084	1.084	1.367	1.371	1.360
R(20–29)	1.199					
R(26–27)		0.963				
R(28–29)		0.963				
R(25–26)			0.963			
R(27–28)			0.963			
R(29–30)			0.983			
R(32–33)				0.962		
R(30–31)				0.966		
R(5–28)				0.963		
R(3–27)				0.993		
R(2–26)				0.966		
R(6–29)				0.966		
R(29–32)				2.194		
R(6–31)				2.179		
R(20–30)				1.357		
R(20–21)				1.398		
R(31–32)					0.966	
R(6–32)					2.133	
R(6–30)					0.962	
R(5–29)					0.963	
R(4–28)					1.692	
R(3–28)					0.993	
R(2–27)					0.965	
R(6–31)						0.963
R(5–30)						0.963
R(4–29)						1.692
R(3–29)						0.993
R(2–28)						0.966

Table 2
Thermo-chemical properties of the selected flavone derivatives were calculated using the DFT/ B3LYP 6311G + + (d) level of theory.

Sample	Energy $\times 10^5$ (kcal/mol)	Molecular Mass (amu)	Enthalpy (H) $\times 10^5$ (kcal/mol)	Gibbs Free Energy (G) $\times 10^5$ (kcal/mol)	Entropy (S) (cal/mol)	ΔH^* $\times 10^5$ (kcal/mol)	$\Delta G^* \times 10^5$ (kcal/mol)	ΔS^* (cal/mol	ΔH^{**} $\times 10^5$ (kcal/mol)	ΔG^{**} $\times 10^5$ (kcal/mol)	ΔS^{**} (cal/mol
Flavone	−4.57	222.07	−4.57	−4.57	112.02						
Chrysin	−5.51	254.06	−5.51	−5.51	123.73	−0.94	−0.94	11.71			
Galangin	−5.98	270.05	−5.98	−5.98	127.25	−1.41	−1.41	15.23			
Kaempferol	−6.45	286.05	−6.45	−6.46	126.80	−1.88	−1.91	14.78	−0.94	−0.48	−0.45
Quercetin	−6.92	302.04	−6.92	−6.92	136.28	−2.35	−2.35	24.26	−1.41	−0.94	9.03
Myricetin	−7.41	318.04	−7.41	−7.41	141.96	−2.84	−2.84	29.94	−1.9	−1.43	14.71

* The relative values in thermodynamic parameter values for each hydroxylated derivative of flavone.
** These deviations represent the thermodynamic parameter differences due to ring B hydroxylation of galangin.

relative binding affinities and thermodynamic characteristics of the selected samples, potentially impacting their biological activities. With an increase in the number of hydroxyl groups, negative deviations in both ΔH* and ΔG* were observed, indicating that the binding process may require more energy input or be less likely to occur spontaneously, potentially resulting in lower binding affinity or efficacy. Conversely, positive ΔS* deviations suggest an increase in entropy, indicating greater disorder or randomness in the system, which could affect binding dynamics. However, focusing on hydroxylation at ring B on galangin, negative values for ΔH** and ΔG** imply weaker binding interactions and less favorable energetics, potentially leading to reduced stability of the flavonoid-target complex. Positive ΔS** values indicate increased disorder during binding, impacting binding dynamics. Additionally, the negative ΔS** value suggests decreased disorder compared to the reference compound, potentially influencing binding dynamics differently than observed for other derivatives.

Frontier molecular orbital analysis (FMO)

The FMOs especially the Highest Occupied Molecular Orbitals (HOMO) and Lowest Unoccupied Molecular Orbitals (LUMO) of the molecules under study were deliberated using the DFT/ B3LYP 6311G + + (d) level of theory and tabulated in Table 3. The HOMO designates the best possible place for an electrophilic attack and their energy signifies the ionization potential of the molecule. The LUMO indicates the greatest probable site which would endure a nucleophilic attack and their energy resembles to electron affinity. A great HOMO–LUMO energy gap signposts better stability and little reactivity of the chemical compound. Based on the frontier molecular orbital analysis, flavone −6.617 eV energy for HOMO and is found to decrease with hydroxylation at positions 5 and 7 in ring A (chrysin) and at position 3 in ring C and reached a less negative value for −5.787 for galangin. On further hydroxylation at ring B (kaempferol), it is found to decrease from −5.787 to −5.93 eV then found to increase to −5.8 ev for quercetin and myricetin. Hence, we can consider galangin and myricetin have tendency for electrophilic attack. Chrysin and kaempferol have a higher propensity for nucleophilic attack when taking into account the assessment of LUMO. The band gap case has the identical HOMO effect; galangin and myricetin have lower energy values.

Global descriptive parameters

For a profound understanding of the reactivivity of certain phytochemical compounds, the global descriptive parameters like hardness, softness, chemical potential, electronegativity, and electrophilicity index were calculated using Koopman's theorem for closed-shell compounds, as follows [16,26].

Ionization potential (IP) $\approx -E_{HOMO}$.

Electron affinity (EA) $\approx -E_{LUMO}$.

where E_{HOMO} is the energy of HOMO and E_{LUMO} is the energy of LUMO.

Hardness (η) $\approx .\frac{IP-EA}{2}$

Electronegativity (χ) $\approx .\frac{IP+EA}{2}$

Softness (S) $\approx .\frac{1}{2\eta}$

Chemical potential (μ) $\approx -\chi$.

Electrophilicity index (ω) $\approx .\frac{\mu^2}{2\eta}$

the derived global descriptors of the flavone derivatives are given in Table 4.

The maximum hardness principle states that, for a given external potential, a molecule's stability increases with hardness and decreases with softness, and that as stability increases, reactivity decreases. These calculated descriptors point out that the flavone has the highest stability and lowest reactivity. The stability is found to decrease on hydroxylation. Again the results emphasize that the single hydroxylation at position 4′ of the B ring has an adverse effect on the reactivity of the molecule. Then additional hydroxylation at ring B again increases the reactivity. Ionization energy is a significant sign of molecule's chemical reactivity. High constancy and chemical inertness are specified by high ionization energy, whereas high reactivity of the atoms and molecules is indicated by low ionization energy. Electron affinity is the capacity of a ligand to accept one electron from a donor. If the electronic chemical potential is higher, the molecule is either less stable or more reactive. The electrophilicity index gauges a species' propensity to receive electrons. On the other hand, a good nucleophile has a low value while a decent electrophile has a great value. Henceforth matching the local descriptors of all flavone derivatives under study, we can infer that quercetin is reactive with a lower electrophilicity index and higher softness index, and smaller hardness value.

Table 3
Frontier molecular orbital of the selected flavone derivatives was calculated using the DFT/ B3LYP 6311G + + (d) level of theory.

Sample	HOMO (eV)	LUMO (eV)	HOMO-1 (eV)	LUMO + 1 (eV)	BAND GAP (eV)
Flavone	−6.62	−2.06	−6.75	−1.13	4.55
Chrysin	−6.27	−1.79	−6.38	−0.80	4.48
Galangin	−5.79	−1.87	−6.73	−0.78	3.92
Kaempferol	−5.93	−1.57	−6.66	−1.01	4.36
Quercetin	−5.85	−1.85	−6.43	−0.79	4.00
Myricetin	−5.86	−1.88	−5.86	−0.74	3.98

Molecular electrostatic potential map (MEP)

For the purpose of molecular electrostatic potential (MEP) mapping, reactive sites for electrophilic and nucleophilic assault must be predicted, one can locate the most electronegative and electropositive site on a compound's skeleton as well as to comprehend the three-dimensional charge dispersals over the compounds in these phytochemicals. The MEP maps of all selected samples were calculated using DFT DFT/ B3LYP 6311G + + (d) level of theory as shown in Fig. 3. It is possible to classify the blue and red zones as nucleophilic and electrophilic reactivity regions, respectively. Zero potential is the designation given to the white areas. It is noteworthy that the neighbourhood of all oxygen atoms is the negative zone for the electrophilic assault, indicating a proton's attraction, while the vicinity of hydroxyl groups indicates a nucleophilic site's attraction to electrons. In flavone, the most electronegative site is concentrated around the ketone group in the pyran ring, due to the presence of lone pair electrons of the oxygen atom, and the electropositivity is shared equally by all other hydrogen atoms in the 3 rings.

Hydroxylation at positions 5 and 7 of ring A in chrysin results in the aggregation of proton density, creating two additional electropositive regions. Interestingly, in kaempferol, just by a single hydroxylation at ring B, the electro positivity from the 5th position of ring A is drifted towards the new OH group by delocalization of electrons from the ring A to benzene ring B through pyran ring C. This delocalization of electrons makes two additional electronegative regions at ring A. The molecular electrostatic potential on the MEP surfaces of the molecules kaempferol, quercetin, and myricetin differs dramatically with increasing the number of hydroxyl groups on the B ring. The distribution of the positive and negative molecular electrostatic potential is not readily apparent in flavone, chrysin, or galangin because none of the hydroxyl oxygen atoms are attached to the B ring. But as the number of hydroxyls increases, Fig. 3 illustrates how the positive electrostatic potential is distributed close to the hydroxyl hydrogen atoms and the negative electrostatic potential is found close to the hydroxyl oxygen atom. Quercetin has two hydroxyl groups attached to it; during additional hydroxylation in myricetin, the negative electrostatic potential energy around the hydroxyl oxygen atom is seen to diminish. These geometric confirmations of these molecules may vary at the time of interaction with targeted

Table 4
Calculated global descriptors of the flavone derivatives under study were calculated using the DFT/ B3LYP 6311G + + (d) level of theory.

	Ionization Potential (IP)	Electron Affinity (EA)	Hardness (η)	Electro-negativity (χ)	Softness (S)	Chemical Potential (μ)	Electrophilicity Index (ω)
Flavone	6.22	2.06	2.28	4.34	0.22	−4.34	4.14
Chrysin	6.27	1.79	2.24	4.03	0.22	−4.03	3.63
Galangin	5.79	1.87	1.96	3.83	0.26	−3.83	3.74
Kaempferol	5.93	1.57	2.18	3.75	0.23	−3.75	3.23
Quercetin	5.85	1.85	2.00	3.85	0.25	−3.85	3.71
Myricetin	5.86	1.88	1.99	3.87	0.25	−3.87	3.76

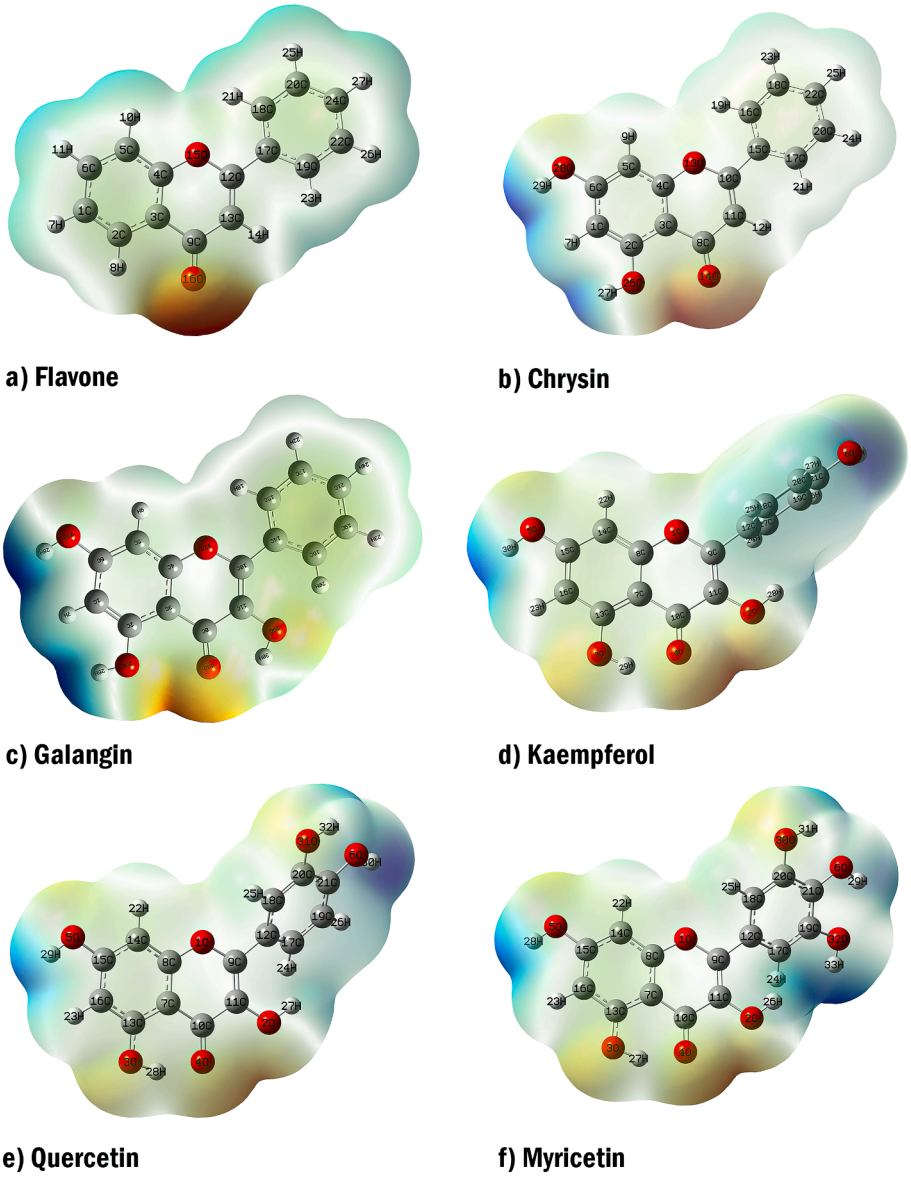

Fig. 3. The MEP structures of a) flavone, b) chrysin, c) galangin and d) kaempferol e) quercetin and f) myricetin. The negative (red) regions of MEP were related to electrophilic reactivity and the positive (blue) regions to nucleophilic reactivity (For interpretation of the references to colour in this figure legend, the reader is referred to the web version of this article).

protein according to their electrophilic and nucleophilic behavior of the active site.

Molecular docking

In this work, all the selected flavones and flavonols are docked to the estrogen receptors, ERα and ERβ, which are inclusive pretty analogous in physiological structure to estradiol. Though estradiol (E2) is not the main circulating estrogen, it is one of the utmost effective endogenous estrogens and has almost similar binding affinity for human ERα and ERβ. Estradiol is used to bind to the estrogen receptor by means of hydrogen bonding. The hydroxyl groups of A ring in estradiol interact with GLU353 and ARG394 and D-ring hydroxyl bonds with HIS524 in addition to the water molecules in the binding pocket. The active site may lock estradiol-like complex phytoestrogen compounds since there is a fair amount of empty space in the binding pocket. Hypothetically, the

selected flavones and flavonols are docked to the binding pocket of estrogen receptors.

Molecular docking studies with ERα

The docking of the inbuilt ligand, estradiol, and the selected samples under study into the 3D structure of ERα was done using a glide dock and the docking score and binding energy were tabulated in Table 5. The residues of amino acids found in the active site of 3ERT are TRP383, LEU384, LEU387, MET388, GLY390, LBU391, VAL392, ARG394, MET342, MET343, LEU345, LEU346, THR347, ASN348, LEU349, ALA350, SP351, GLU353, LEU354, LEU327, PHE404, LEU402, LEU428, PHE425, ILE424, VAL422, MET421, GLY420, GLU419, VAL418, MET517, SER518, LYS520, GLY521, MET522, GLU523, HIE524, LEU525, MET528, LYS529, CYS530, VAL533, LEU536, LEU539. In which the inbuilt ligand estradiol docks into the active site region and interacts with the residues by hydrogen bonding with GLU353 and ARG394 and electrostatic bonding with ASP351. The inbuilt ligand shows a docking score of −12.17 and binding energy of −125.19 kcal/mol. The docking results emphasize that the active site of ERα is an electrophile site, which dislikes hydroxyl groups. Hence, as hydroxylation increases, it is found to repel from the site with a decrease in docking score. It is also found that chrysin docks well to the active site of ERα with a docking score −8.516 and binding energy −48.251 kcal/mol and it was found to decrease on hydroxylation and reaches to a minimum for quercetin and myrecetin. The 3D and 2D figures of other ligands are given in Fig. 4. The docking score and binding energy of other ligands are given in table.

The 2D interaction picture of ERα (Fig. 5) reveals the type of interaction between the ligands and amino acids in the active sites of ERα. The inbuilt ligand estradiol forms hydrogen bond with GLY420, ARG 394, and GLU353. At the same time, flavone lacks any bonding, chrysin makes a single hydrogen bond with LEU346, galangin with GLU353, kaempferol, quercetin, and myricetin with ASP351.

Molecular docking studies with ERβ

The amino acid residues in the active site of ERβ (PDBID: 3OLL) are VAL280, MET295, SER297, LEU298, THR299, LEU301, ALA302, ASP303, GLU305, TRP335, MET336, LEU339, MET340, GLY342, LEU343, MET344, ARG346, LEU354, PHE356, VAL370, GLY372, ILE373, ILE376, PHE377, LEU380, ALA468, SER469, LYS471, GLY472, MET473, HIE475, LEU476, LEU477, MET479, VAL485, LEU491, LEU495 (Fig. 6). The inbuilt ligand is bound deep into the dynamic site area, making hydrogen bonding dealings with HIE475, ARG346, GLU305, and π-π stacking interactions with PHE356 (Fig. 7). The inbuilt ligand shows a docking score −10.7 and binding energy of −87.155 kcal/mol. Flavone has the least docking score and binding affinity towards ERβ due to the lack of OH functional groups. As hydroxylation increases it is found to increase the binding affinity and docking score till quercetin. The docking results emphasize that the active site of ERβ is a nucleophile site, which is hydroxyl loving site. The docking of ERβ with quercetin shows the highest docking score of −9.120 and binding energy of −64.927 kcal/mol (Table 5).

Table 5
Docking score and binding affinity of selected flavone derivatives with ERα and ERβ.

Sample	ERα		ERβ	
	Docking Score	Binding Energy kcal/mol	Docking Score	Binding Energy kcal/mol
Inbuilt ligand estradiol	−12.17	−125.17	−10.71	−87.15
Flavone	−7.73	−48.25	−7.69	−52.16
Chrysin	−8.52	−50.21	−8.31	−57.36
Galangin	−7.35	−45.20	−8.27	−57.69
Kaempferol	−6.97	45.15	−8.58	−59.28
Quercetin	−6.99	−47.12	−9.12	−64.92
Myricetin	−5.68	−50.92	−8.15	−37.34

Discussion

Flavonoids, which consist of a 15-carbon skeleton comprising two phenyl rings (A and B) and a heterocyclic ring (C), are biosynthesized by plants and undergo various modifications through microbial transformations and other metabolic processes. This results in a wide range of flavonoid subtypes, each with distinct biological activities. Remarkably, flavonoids are reported to exert their effects on biological systems primarily by interacting with estrogen receptors (ER) and modulating downstream signaling pathways. However, controversy exists regarding the chemical nature of phytoestrogens, their interactions with receptors, and the complex physiological perspectives in which they operate. Several factors contribute to the intricate nature of phytoestrogens, including structural diversity, the dynamics of agonist–antagonist actions, tissue-specific effects, dose dependency, and individual variations. In particular, the dual nature of these compounds, which can act as either agonists or antagonists, makes it challenging to determine their overall impact on estrogen signaling. To unravel this intricate web of interactions, the present study aims to establish a correlation between the binding efficacy of flavonols, a prominent subgroup of flavonoids, and the hydroxylation pattern on ring B using *in silico* methods.

Breast cancer exhibits varying clinical behaviors due to its heterogeneity primarily driven by histological variations, molecular subtypes, genetic diversity, and the tumor microenvironment. One crucial aspect of molecular subtypes is the presence of estrogen receptors, particularly ERα and ERβ which largely influence on the effect of phytoestrogens. Studies have suggested the role of ERβ in supressing tumour development especially in breast. The knockdown of ERβ is found to increase the proliferation of breast cancer cells, whereas its overexpression inhibited the growth. ERβ possessing breast cancer cell type MDA-MB 453, is reported to inhibit the proliferation by suppressing PI3K/AKT pathway through PTEN [28]. A relation of ERβ and P53 function is also suggested [29]. Thus, the role of ERβ in cellular metabolism and regulation revealed by a number of studies might be the attractive targets to pursue in triple negative breast cancer (TNBC) management [27,28,30]. Phytoestrogens are considered as the natural agonists of ERβ and are largely enticed as promising drug candidates due to their role in modulating cell cycle, epigenetic events and inducing apoptosis.

Accordingly, the molecular docking results of the present study emphasize a notable preference among the selected phytoestrogens for binding to ERβ over ERα. This preference could be attributed to the nuanced differences in the ligand binding sites of these two estrogen receptors. While it is important to note that ERα and ERβ are the products of distinct genes, it is intriguing that they still exhibit a high degree of similarity, sharing a remarkable 96% homology in their DNA-binding domains and a substantial 60% homology in their ligand binding domains. This intricate balance of shared and distinct structural features may play a pivotal role in dictating the specific affinity of these phytoestrogens towards ERβ, offering valuable insights into the selectivity and potential therapeutic implications of these compounds in modulating estrogen receptor signaling pathways.

The ligand binding sites of ERα and ERβ display a three-layered antiparallel α-helical fold, which is formed with 10–12 helices. The short H1 observed in ERα is absent from both ERβ complexes as the first 7–8 residues at the N-terminus are disordered. In addition, the loop regions connecting H2 and H3 (residues 282–289) and H9 and H10 (410–428) exhibit different conformations in the two structures [31 32]. More specifically, the binding site of ERα has 12 helices. The antiparallel α-helical fold, comprising a central core layer of three helices (H5/6, H9, and H10), is sandwiched between two additional layers of helices (H1-4 and H7, H8, and H11). The remaining secondary structural elements, a small two-stranded antiparallel β-sheet and the dynamically mobile H12 flank the main three-layered motif. This helical arrangement creates a

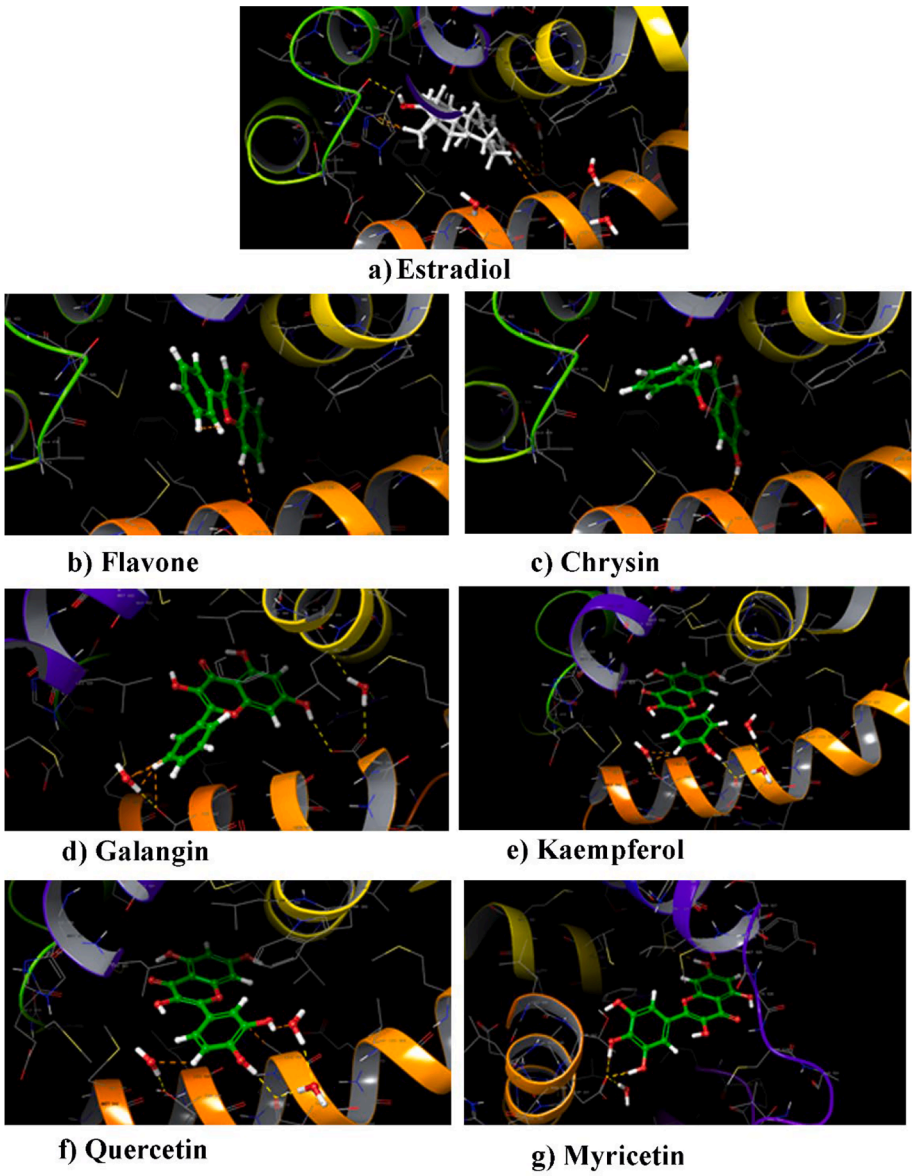

Fig. 4. 3D interaction picture of ERα with the selected flavone derivatives.

scaffold that maintains a ligand-binding cavity. Understandably, the integrity of the coactivator-binding groove is highly dependent on the orientation of H12. In turn, the alignment of H12 is highly sensitive to the nature of the bound ligand. Only those ER ligands that promote the positioning of H12 over the hormone binding cavity will act as full agonists [33]. When estradiol binds to ERα, it locks in the hydrophobic area of the site formed by H3, H6, H8, H11 and H12 and forms nonpolar interactions with the hydrophobic residues. In addition, the phenolic hydroxyl group from the A ring forms hydrogen bonds with GLU353 in H3 and ARG394 in H6 while the 17 hydroxyl group of the D ring forms a hydrogen bond with HIS524 (H11) [31]. A similar observation has been obtained in this work too (Fig. 6), estradiol docks with a docking score of −12.172 and binding energy −125.17 kcal/mol. But, when the selected flavonoids tried to bind, the size of ligand is not compatible with the cavity, when the inner hydrophobic surface of helix H12 to be positioned across H3 and H11 thus forming a lid over the cavity to accommodate co-regulator binding. Any how, flavone docks with ERα with a docking score of −7.730 and binding energy −48.251 kcal/mol, but on hydroxylation of flavone in ring B prevents the hydrophobic interactions of H12 with H3/H11 thus attaining an inactive/open conformation (Fig. 6). And thus docking score reduced to −5.6 for myricetin. As on hydroxylation of flavonoid on ring B the antagonist nature towards ERα is found to increase.

Conversely, in ERβ, the loop regions connecting H2, H3, H9 and H10 are not involved in intermolecular contacts, the loop connecting H9 and H10 is poorly ordered and the N-terminal end of H10 is foreshortened. Further, the N-terminal end of H5 (383–384) is shifted away from H3 and towards H9 and *H*10 effecting the positioning of the side chains of LEU 384 and TRP 383 [32]. The volume of the probe occupied ligand pocket of ERβ is reduced being primarily due to the replacement of the LEU384 and TRP383 in ERα with bulkier HIE 475 and MET336 residue in ERβ. This allows the residues that line the pocket to pack more tightly around the flavonoids, stabilizing the ligand in the binding pocket in ERβ. Moreover, the ligands forms p interaction with PHE356. As on hydroxylation, the binding affinity is increasing due to the polar intearaction between the hydrophobic site and ligand is possible. The polar interaction between the ligands and ligand binding site of ERα is negligible due to inactive nature due to open confirmation of the cavity and bulk empty space. At the same time the reduction in cavity size of ERβ and the replacement of LEU384 with polar HIE475 and MET336 increased the polarity and hydrophilicity of the cavity and lead to electrostatic interaction between the docked ligands and the amino acid,

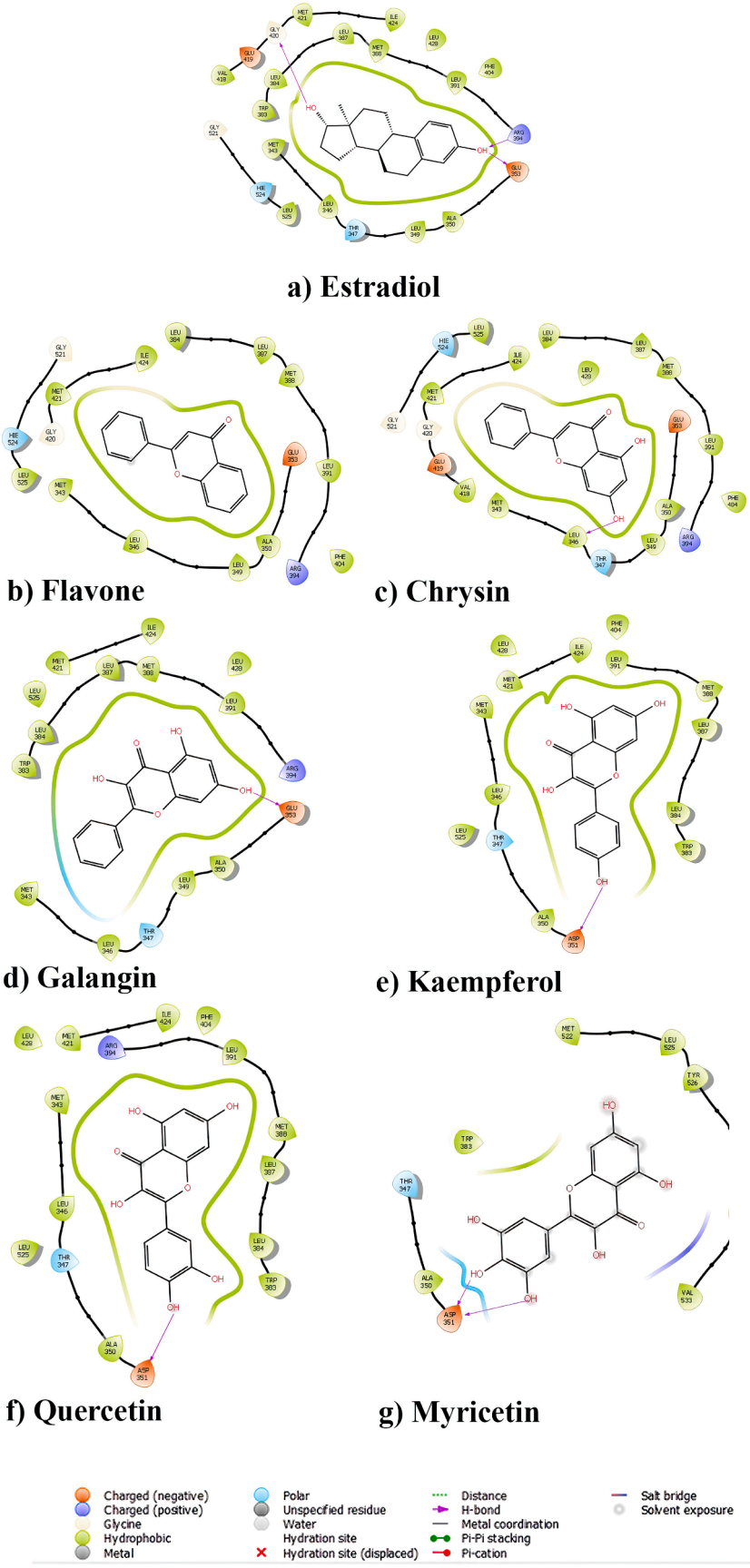

Fig. 5. 2D interaction picture of ERα with the selected flavone derivatives.

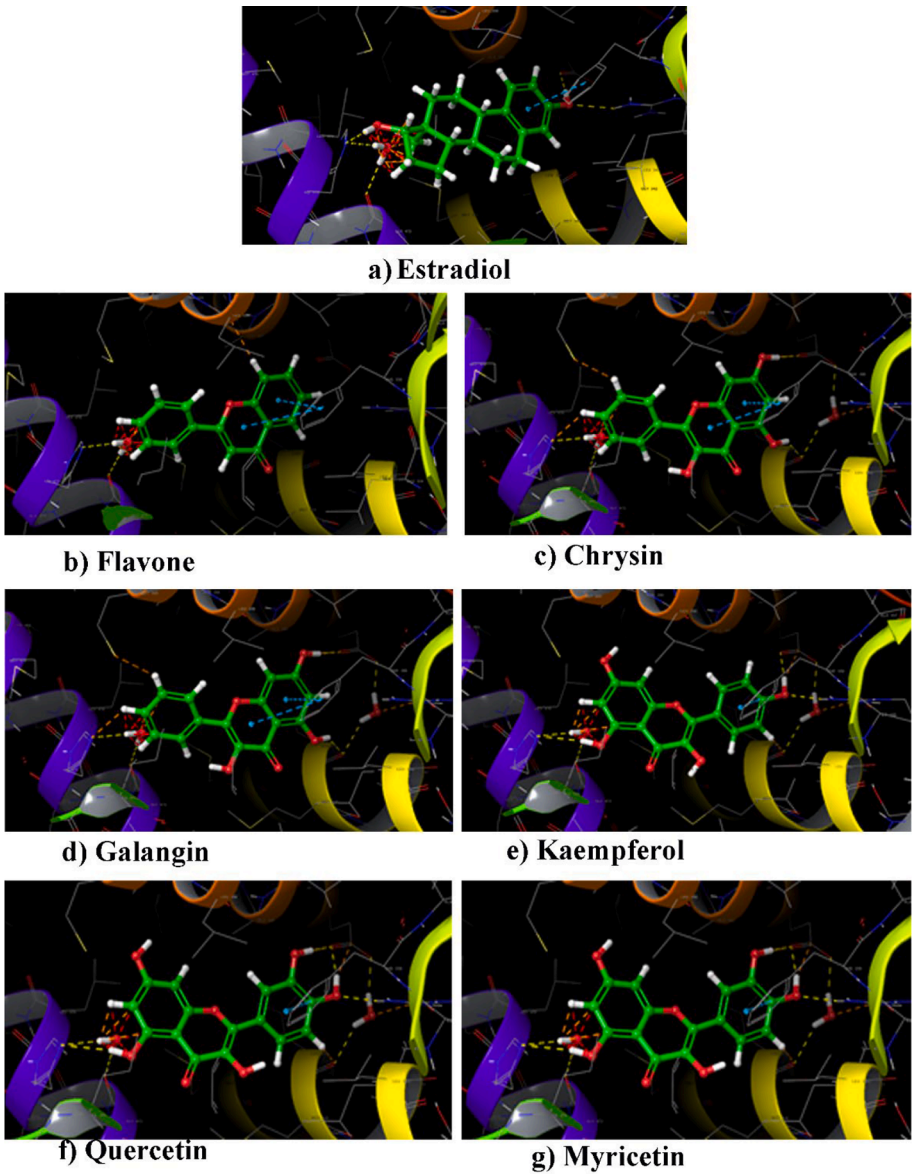

Fig. 6. 3D interaction picture of ERβ with the selected flavone derivatives.

reflected in the colouration of salt bridge. Hence on hydroxylation the of flavonoid increases the binding affinity in ERβ than ERα. The active site in ERα is found to be hydrophobic while ERβ is hydrophilic.

All these experiments discussed earlier emphasised that the number of hydroxyl groups, especially those on the B ring of the flavonoid, seems to be important, whereas changes in A- or C-ring hydroxylation are of minor importance [7]. On the basis of that, the quantum mechanical calculations were done to predicts that the chemical reactivity of the flavonoids. The results emphasised similar to other studies, we found that a hydroxyl group at position 3 and 5 in ring A and C are relevant, in addition, hydroxylation on ring B have significant importance in the chemical reactivity as well as estrogenic activity. The calculated Gibbs free energy and entropy points out that the most stable compound among the selected compounds is flavone and the least stable and more reactive is quercetin and myricetin, both have more or less same value. The results are supported by the electronic configuration of frontier molecular orbitals, which shows that myrceitin and quercitin require less energy to activate. According to the precise insight to the frontier molecular orbitals with Koopman's theorem draws some controversial results, the ionization potential, hardness, and softness values indicate to galangin as the most reactive molecule, comparable to quercetin and myricetin. Additionally, kaempferol's reactive nature is also supported by the computed values for electron affinity, electronegativity, chemical potential, and electrophilicity index. The MEP map suggests that the molecular structure of flavone is neutral lacking electronegative and electropositive sites. However, on hydroxylation the electropositive and electronegative area on the molecule is found to increase and reaches a maximum for quercetin after that it is found to diminish. Hence from all these quantum mechanical results we may draw attention towards quercetin as most chemically reactive molecule and flavone as the least reactive one.

Thus the relationship between the number of hydroxyl groups in flavonoids and their binding affinity on ERβ and ERα reveals an intriguing controversy. This phenomenon can be attributed to two key factors. Firstly, when hydroxylation occurs at ring B of flavone, it leads to an increase in both electropositive and electronegative regions within the molecule. Secondly, the structural variations in the ligand binding sites of estrogen receptors play a pivotal role. Notably, the binding site of ERα is characterized by an inactive nature due to its open cavity confirmation and substantial empty space. Conversely, in ERβ, the substitution of polar residues like HIE475 and MET336 for LEU384 enhances the polarity and hydrophilicity of the cavity. Consequently,

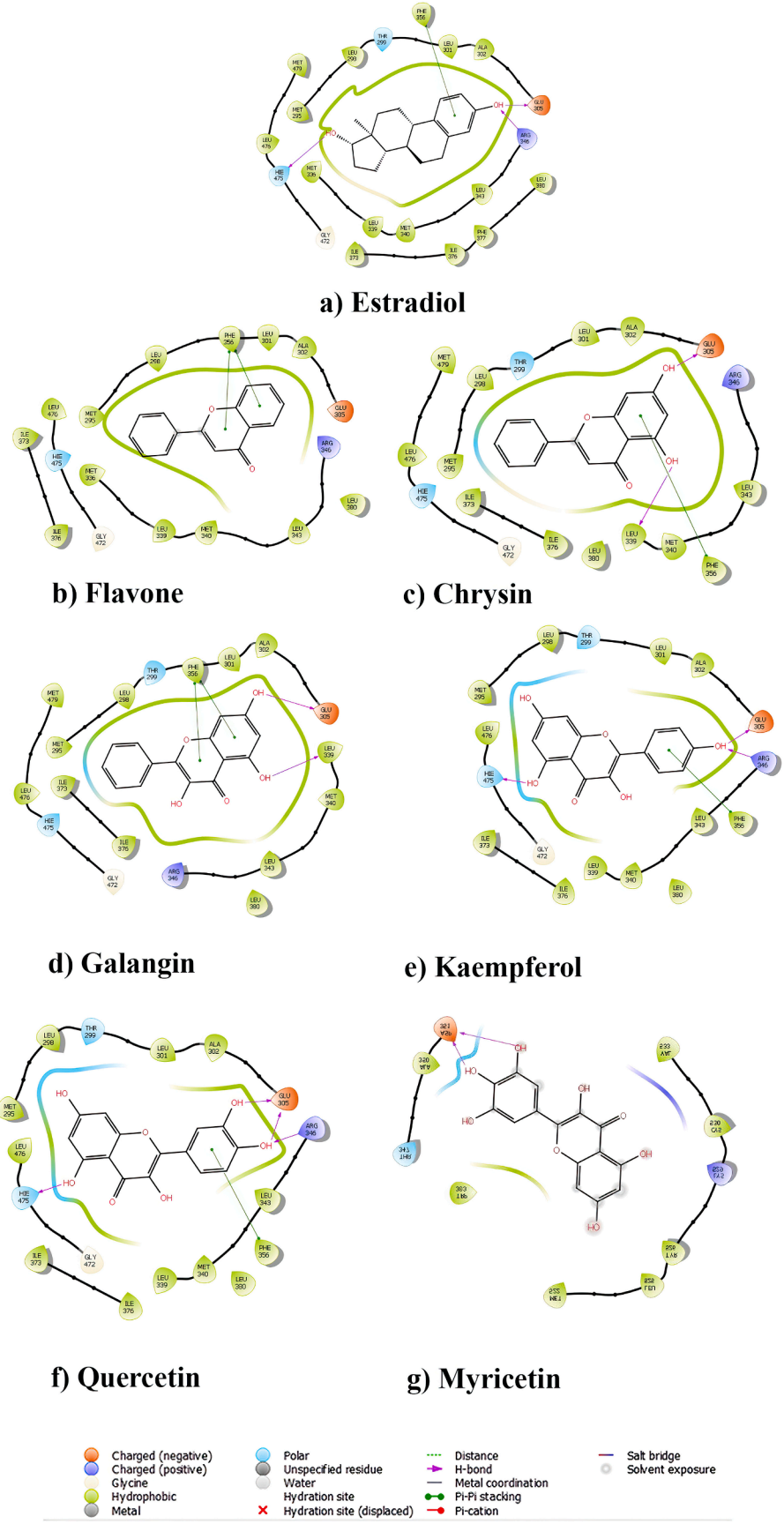

Fig. 7. 2D interaction picture of ERβ with the selected flavone derivatives.

this alteration facilitates polar interactions between flavonoids and the ligand binding site, leading to an increase in efficacy as the number of hydroxyl groups on the flavonoids increases. These findings align well with experimental results on phytoestrogens, indicating that they exhibit stronger competition with estradiol for binding to ERβ compared to ERα.

Conclusion

In conclusion, the study focuses the importance of the hydroxylation pattern on ring B in determining the affinity and efficacy of flavonols towards estrogen receptors. Specifically, the presence of a hydroxyl group on ring B was associated with increased binding affinity and efficacy, highlighting the crucial role of this structural feature in modulating estrogen receptor interactions. The results elucidate the distinct hydrophilic nature of the ERβ binding site, showcasing enhanced electrostatic interactions with flavonols possessing specific hydroxyl configurations. Conversely, ERα exhibited a hydrophobic environment with less polar interactions due to its open cavity conformation. Overall, these insights deepen our understanding of flavonol-estrogen receptor interactions, emphasizing the pivotal role of ring B hydroxylation in both chemical reactivity and estrogenic activity within this class of compounds.

CRediT authorship contribution statement

K.P Safna Hussan: Writing – original draft, Conceptualization. **Anu Davis:** Formal analysis, Data curation. **S. Lekshmi:** Investigation, Funding acquisition. **Mohamed Shahin Thayyil:** Software, Resources, Methodology. **Achuthan Chathrattil Raghavamenon:** Writing – review & editing. **Thekkekara Devassy Babu:** Writing – review & editing, Writing – original draft.

Declaration of competing interest

The authors declare the following financial interests/personal relationships which may be considered as potential competing interests: KP SAFNA HUSSAN reports financial support was provided by Council of Scientific & Industrial Research (CSIR) for the RA fellowship with file no: 09/0869/ (1169)/EMR-1–2021 in Amala Cancer Research Center. KP SAFNA HUSSAN reports a relationship with Amala Cancer Research Center that includes: employment and funding grants. KP SAFNA HUSSAN has patent #202341024745 pending to Amala Cancer Research Center.

Acknowledgments

Authors thankfully acknowledge the Central Sophisticated Instrument Facility (CSIF) of University of Calicut for providing Schrodinger Maestro software and hardware support. KPSH acknowledges Council of Scientific & Industrial Research (CSIR) for the RA fellowship with file no: 09/0869/(1169)/EMR-1-2021 in Amala Cancer Research Center.

References

[1] H.H. Al Mamari, Phenolic Compounds: Classification, Chemistry, and Updated Techniques of Analysis and Synthesis, in: Intech, 2016: p. 13. https://www.intechopen.com/books/advanced-biometric-technologies/liveness-detection-in-biometrics.

[2] S. Huang, B. Qi, L. Yang, X. Wang, J. Huang, Y. Zhao, Y. Hu, W. Xiao, Phytoestrogens, novel dietary supplements for breast cancer, Biomed. Pharmacother. 160 (2023) 114341, https://doi.org/10.1016/j.biopha.2023.114341.

[3] A.N. Panche, A.D. Diwan, S.R. Chandra, Flavonoids: An overview, J. Nutr. Sci. 5 (2016) 1–15, https://doi.org/10.1017/jns.2016.41.

[4] V.J. Ankur Kumar Tanwar, Neha Dhiman, Amit Kumar, Engagement of phytoestrogens in breast cancer suppression: Structural classification and mechanistic approach, Eur J Med Chem. 213 (2021) 113037.

[5] V. Breinholt, J.C. Larsen, Detection of weak estrogenic flavonoids using a recombinant yeast strain and a modified MCF7 cell proliferation assay, Chem. Res. Toxicol. 11 (1998) 622–629, https://doi.org/10.1021/tx970170y.

[6] T.J. Murray, X. Yang, D.H. Sherr, Growth of a human mammary tumor cell line is blocked by galangin, a naturally occurring bioflavonoid, and is accompanied by down-regulation of cyclins D3, E, and A, Breast Cancer Res. 8 (2006) 1–12.

[7] A. Resende, A.P.S. De Oliveira, M.S. De Camargo, W. Vilegas, Evaluation of estrogenic potential of flavonoids using a recombinant yeast strain and MCF7 / BUS cell proliferation assay, PLoS One 8 (2013) 1–7, https://doi.org/10.1371/journal.pone.0074881.

[8] G.G.J.M. Kuiper, J.G. Lemmen, B. Carlsson, J.C. Corton, S.H. Safe, P.T. Van Der Saag, B. Van Der Burg, J.Å. Gustafsson, Interaction of estrogenic chemicals and phytoestrogens with estrogen receptor β, Endocrinology 139 (1998) 4252–4263, https://doi.org/10.1210/endo.139.10.6216.

[9] H.K.B. Sarah M Mense, Tom K Hei, Ramesh K Ganju, Phytoestrogens and breast cancer prevention: possible mechanisms of action, Env. Heal. Perspect. 4 (2008) 33.

[10] D.M. Kopustinskiene, V. Jakstas, A. Savickas, J. Bernatoniene, Flavonoids as anticancer agents, Nutrients 12 (2020) 1–24, https://doi.org/10.3390/nu12020457.

[11] R. Kubina, M. Iriti, A. Kabała-Dzik, Anticancer potential of selected flavonols: Fisetin, kaempferol, and quercetin on head and neck cancers, Nutr. Rev. 13 (2021) 1–20.

[12] E.E. Bolton, Y. Wang, P.A. Thiessen, S.H. Bryant, Integrated Platform of Small Molecules and Biological Activities, in: R.A.W. and D.C.S.B.T.-A.R. in C. Chemistry (Ed.), Elsevier, 2008: pp. 217–241. doi: https://doi.org/10.1016/S1574-1400(08)00012-1.

[13] N.M. O'Boyle, M. Banck, C.A. James, C. Morley, T. Vandermeersch, G. R. Hutchison, Open Babel: An open chemical toolbox, J. Chem. Informatics 3 (2011) 33.

[14] M.J. Frisch, G.W. Trucks, H.B. Schlegel, G.E. Scuseria, M.A. Robb, C. J.R., G. Scalmani, V. Barone, B. Mennucci, G.A. Petersson, H. Nakatsuji, M. Caricato, X. Li, H.P. Hratchian, A.F. Izmaylov, J. Bloino, G. Zheng, J.L. Sonnenberg, M. Hada, M. Ehara, K. Toyota, R. Fukuda, J. Hasegawa, M. Ishida, T. Nakajima, Y. Honda, O. Kitao, H. Nakai, E. T. Vreven, J.A. Montgomery, Jr., J.E. Peralta, F. Ogliaro, M. Bearpark, J.J. Heyd, A. Brothers, K.N. Kudin, V.N. Staroverov, R. Kobayashi, J. Normand, K. Raghavachari, M.K. Rendell, J.C. Burant, S.S. Iyengar, J. Tomasi, M. Cossi, N. Rega, J.M. Millam, R.E.S. J.E. Knox, J.B. Cross, V. Bakken, C. Adamo, J. Jaramillo, R. Gomperts, K.M. O. Yazyev, A.J. Austin, R. Cammi, C. Pomelli, J. Ochterski, R.L. Martin, O. V.G. Zakrzewski, G.A. Voth, P. Salvador, J.J. Dannenberg, S. Dapprich, A.D. Daniels, D.F. Farkas, J.B. Foresman, J. V. Ortiz, J. Cioslowski, J., GAUSSIAN 09 (Revision A.2) Gaussian, Inc., Wallingford, CT, D. J. Gaussian 09,. B.01; (1998).

[15] V.K. Rajan, K. Muraleedharan, A computational investigation on the structure, global parameters and antioxidant capacity of a polyphenol, Gallic acid, Food Chem. 220 (2017) 93–99, https://doi.org/10.1016/j.foodchem.2016.09.178.

[16] Safna Hussan K P, Mohamed Shahin Thayyil, Vijisha K Rajan, Muraleedharan K, Experimental and density functional theory studies on benzalkonium ibuprofenate, a double active pharmaceutical ingredient, Comput. Biol. Chem. 72 (2018) 113–121. doi: 10.1016/j.compbiolchem.2017.12.004.

[17] K.P.S. Hussan, M.S. Thayyil, V.K. Rajan, K. Muraleedharan, DFT studies on global parameters, antioxidant mechanism and molecular docking of amlodipine besylate, Comput. Biol. Chem. 80 (2019) 46–53, https://doi.org/10.1016/j.compbiolchem.2019.03.006.

[18] K.P.S. Hussan, M.S. Thayyil, S.K. Deshpande, T.V. Jinitha, V.K. Rajan, K.L. Ngai, Synthesis and molecular dynamics of double active pharmaceutical ingredient-benzalkonium ibuprofenate, J. Mol. Liq. 223 (2016) 1333–1339, https://doi.org/10.1016/j.molliq.2016.09.054.

[19] K.G. Sangeetha, K.K. Aravindakshan, K.P.S. Hussan, Insight into the theoretical and experimental studies of 1-phenyl-3- phenylthiosemicarbazone - A potential NLO material, J. Mol. Struct. 1150 (2017) 135–145, https://doi.org/10.1016/j.molstruc.2017.08.078.

[20] K.P. Safna Hussan, T. Mohamed Shahin, S.K. Deshpande, T. V Jinitha, Photoluminescent behavior of propylene carbonate and poly (methylmethacrylate) blend for transparent optoelectronic devices, AIP Conf. Proc. 1849 (2017) 020012-1–6. doi: 10.1063/1.4984159.

[21] K.P. Safna Hussan, T. Mohamed Shahin, M. Binesh, S.K. Deshpande, V.K. Rajan, Molecular dynamics in amorphous pharmaceutically important protic ionic liquid – benzalkonium chloride, J. Mol. Liq. 251 (2018) 487–491, https://doi.org/10.1016/j.molliq.2017.12.007.

[22] M. Szermerski, J. Melesina, K. Wichapong, M. Löppenberg, J. Jose, W. Sippl, R. Holl, Synthesis, biological evaluation and molecular docking studies of benzyloxyacetohydroxamic acids as LpxC inhibitors, Bioorg. Med. Chem. 22 (2014) 1016–1028, https://doi.org/10.1016/j.bmc.2013.12.057.

[23] T. Schulz-Gasch, M. Stahl, Binding site characteristics in structure-based virtual screening: evaluation of current docking tools, J. Mol. Model. 9 (2003) 47–57, https://doi.org/10.1007/s00894-002-0112-y.

[24] S. Aktar, M.F. Khan, M.M. Rahman, M.A. Rashid, Computational study of geometry, polarizability, hyperpolarizability and molecular docking studies of naproxen, Dhaka Univ. J. Pharm. Sci. 15 (2016) 37–45, https://doi.org/10.3329/dujps.v15i1.29191.

[25] M. Spiegel, T. Andruniów, Z. Sroka, Flavones' and flavonols' antiradical structure–activity relationship—a quantum chemical study, Antioxidants 9 (2020) 461–483, https://doi.org/10.3390/antiox9060461.

[26] K.G. Sangeetha, K.K. Aravindakshan, K.P. Safna Hussan, Insight into the theoretical and experimental studies of 1-phenyl-3-methyl-4-benzoyl-5-pyrazolone N (4)-

methyl- N (4)- phenylthiosemicarbazone - A potential NLO material, J. Mol. Struct. 1150 (2017) 135–145. doi: 10.1016/j.molstruc.2017.08.078.
[27] E.K. Shanle, Z. Zhao, J. Hawse, K. Wisinski, S. Keles, M. Yuan, Research resource: Global identification of estrogen, Res. Resour. 27 (2013) 1762–1775, https://doi.org/10.1210/me.2013-1164.
[28] A. Anestis, C. Mihailidou, S. Theocharis, D. Tryfonopoulos, A. Korogiannos, A. Koumarianou, E. Xingi, M. Kontos, A.G. Papavassiliou, M. V Karamouzis, The predictive role of estrogen receptor beta (ER-β) in androgen receptor (AR)-positive triple-negative breast cancer (TNBC), Abstr. B. Int. Congr. Target. Anticancer Ther. 2018 5-7 March, Paris, Fr. 29 (2018) iii32. doi: 10.1093/annonc/mdy047.087.
[29] I. Bado, F. Nikolos, G. Rajapaksa, J.-åke Gustafsson, ERβ decreases the invasiveness of triple-negative breast cancer cells by regulating mutant p53 oncogenic function, Oncotarget. 7 (2016) 19–21.
[30] N. Hamilton, D. Márquez-garbán, V. Mah, G. Fernando, Y. Elshimali, H. Garbán, D. Elashoff, J. Vadgama, L. Goodglick, R. Pietras, Biologic Roles of Estrogen Receptor-β and Insulin-Like Growth Factor-2 in Triple-Negative Breast Cancer, 2015 (2015).
[31] A. Sinyani, K. Idowu, L. Shunmugam, H. Mathambo, R. Khan, F. Group, A molecular dynamics perspective into estrogen receptor inhibition by selective flavonoids as alternative therapeutic options, J. Biomol. Struct. Dyn. 41 (2023) 4093–4105. doi: 10.1080/07391102.2022.2062786.
[32] A.C.W. Pike, A.M. Brzozowski, R.E. Hubbard, T. Bonn, A. Thorsell, O. Engstro, J. Ljunggren, J.-åke Gustafsson, M. Carlquist, Structure of the ligand-binding domain of oestrogen receptor beta in the presence of a partial agonist and a full antagonist Structure of the ligand-binding domain of oestrogen receptor beta in the presence of a partial agonist and a full antagonist, EMBO J. 18 (1999) 4608–4618. doi: 10.1093/emboj/18.17.4608.
[33] D. Austin, N. Hamilton, Y. Elshimali, R. Pietras, Y. Wu, J. Vadgama, Estrogen receptor-beta is a potential target for triple negative breast cancer treatment, Oncotarget 9 (2018) 33912–33930, https://doi.org/10.18632/oncotarget.26089.